Evaluation of ATR-FTIR Spectroscopy with Multivariate Analysis to Study the Binding Mechanisms of ZnO Nanoparticles or Zn2+ to Chelex-100 or Metsorb

ARTICLE *in* ENVIRONMENTAL SCIENCE & TECHNOLOGY · AUGUST 2013

Impact Factor: 5.33 · DOI: 10.1021/es4017552 · Source: PubMed

4 AUTHORS:

Hamid M. Pouran
Lancaster University
12 PUBLICATIONS **39** CITATIONS
SEE PROFILE

Francis L Martin
Lancaster University
233 PUBLICATIONS **4,316** CITATIONS
SEE PROFILE

Valon Llabjani
Lancaster University
23 PUBLICATIONS **403** CITATIONS
SEE PROFILE

Hao Zhang
Lancaster University
191 PUBLICATIONS **6,704** CITATIONS
SEE PROFILE

Environmental Science & Technology

Article

pubs.acs.org/est

Evaluation of ATR-FTIR Spectroscopy with Multivariate Analysis to Study the Binding Mechanisms of ZnO Nanoparticles or Zn^{2+} to Chelex-100 or Metsorb

Hamid M. Pouran,*[,†] Valon Llabjani,[‡] Francis L. Martin,[‡] and Hao Zhang*[,†]

[†]Lancaster Environment Centre, [‡]Centre for Biophotonics, Lancaster University, Bailrigg, Lancaster, LA1 4YQ, U.K.

Supporting Information

ABSTRACT: Advancements in nanotechnology and the expected increases in production of commercial products with incorporated manufactured nanomaterials will very likely lead to increasing contamination of nanoparticles (NPs) in the environment. Though studying adverse impacts of NPs in the environment and their ecotoxicological fate and behavior is not new, limited information is available. A major challenge in this respect is the lack of a proper sampling technique that could provide data on concentrations of these materials in the environment. Diffusive gradient in thin-films (DGT) is a well-established method that can measure available concentrations of trace metals in soils and waters. Using this approach, different binding resins are employed as a sink to collect targeted chemicals during fixed times. Here, we examine the suitability of two common types of the DGT binding agents, commercially available Chelex-100 and Metsorb, to investigate whether these materials could irreversibly retain a model nanoparticle, ZnO, and if so, what would be the difference between bound ZnO NP and Zn^{2+} ion. Attenuated total reflection-Fourier transform infrared (ATR-FTIR) spectroscopy was used to study the binding materials before and after exposure to ZnO NP and Zn^{2+}. Based on computational analysis using principal component analysis and linear discriminant analysis (PCA-LDA), it was demonstrated that both Chelex-100 and Metsorb form chemical bonds with ZnO NP and Zn^{2+}, however the binding mechanisms of these zinc species as inferred from their infrared (IR) spectra are statistically different (95% confidence level). The experimental results suggest that the binding resins hold ZnO NP with fewer and weaker chemical bonds compared to Zn^{2+}. This research shows the potential of the DGT method to measure available concentrations of nanoparticles in the environment and demonstrate how ATR-FTIR spectroscopy, when used with computational analysis, can differentiate between diverse chemical species that are simultaneously retained by the binding layer in a DGT device.

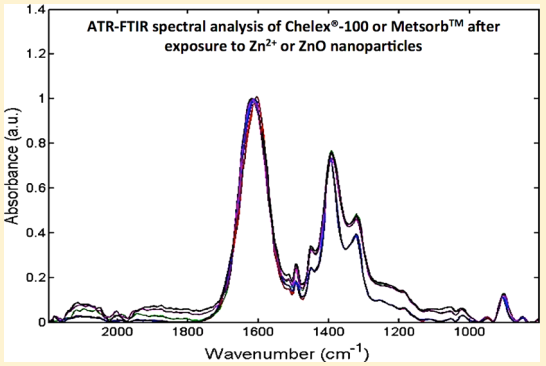

1. INTRODUCTION

Diffusive gradients in thin-films (DGT) is a well-established method to measure time-averaged concentrations of different metal species in soils and waters.[1−3] A DGT device consists of an external filter membrane, a diffusive hydrogel layer and a binding layer. Detailed structure and functions of each component of the DGT device has been previously described.[1] Assuming that metal species are small enough to diffuse though the diffusive layer, they reach the binding resin and are retained by it. Recent investigations have also noted the potential of the DGT technique to measure concentrations of manufactured nanomaterials in the environment.[3] The structure of the DGT device allows to combine different types of diffusive and binding layers and optimize measurements of targeted chemicals. Agarose, open pore and restricted gels and Chelex-100, Metsorb and Fe-Oxide gels are respectively the three common types of diffusive and binding layers used in the DGT technique.[3−6] Although precise pore sizes are unknown, according to some research particles as large as 100 nm are able to pass through open pore diffusive gel.[7]

In this study, we focus on two different types of binding resins, Chelex-100 and Metsorb, which are both commercially available. Chelex-100 function as an ion-exchange resin with roots in its chemical structure that includes dicarboxylic acid amine ($COOHCH_2-NH-COOHCH_2$).[8] Deprotonation of these carboxyl groups that occur in relatively low pH (pH ≈ 4) makes them efficient binding surfaces.[8] Metsorb is mainly a titanium oxide-based material with TiO_2 and $Ti(OH)_4$ as its main constituents. It is known that Metsorb contains a small portion of other chemicals (e.g., polymers) as well, but its detailed chemical structure is not disclosed.[9] Metsorb titanium oxide/hydroxide constituents have a relatively low point of zero charge (the pH that overall surface charge is neutral); these pH values are ≈4.5 for $Ti(OH)_4$ and ≈6.0 for TiO_2.[10,11] This leads to an overall negative surface charge for Metsorb at the pH of most of natural environments. Both Chelex-100 and Metsorb

Received: April 22, 2013
Revised: July 29, 2013
Accepted: August 15, 2013
Published: August 15, 2013

have been used as binding resins for the DGT devices and proven to be effective in measuring targeted chemical concentrations in soil and water.[3,12,13]

While considerable information about the performance of Chelex-100 and Metsorb based DGT devices is available,[6,14] there is no detailed study defining how target chemicals bind to these binding layers. Such information could be used to investigate the potential of the DGT technique to measure different types of targeted chemicals, including manufactured nanomaterials, as a prerequisite to better understand their fate and behavior in the environment.

We set out to investigate the retention mechanism of two different chemicals, Zn^{2+} ion and ZnO nanoparticles (NPs) by Chelex-100 and Metsorb using attenuated total reflection-Fourier transform infrared (ATR-FTIR) spectroscopy. ZnO NP was chosen as our model test agent, because of its extensive applications in industry and commercially available products;[15,16] semiconductors and sunscreen lotions are two examples.[17] In the future, we expect to see growth in manufactured materials that incorporate ZnO NPs. Limited lifetime of these products will increase the risk of their release into different environment compartments.[18] Moreover, toxicological studies have shown ZnO NPs have adverse effects on ecosystems.[19] In parallel to ZnO NP, Zn^{2+} binding behavior was studied because ZnO NP could be dissolved and produce Zn^{2+}.[18] Zn^{2+} by itself is a common metal ion in the environment and it could have toxicological impacts in the environment at high concentrations.[20]

ATR-FTIR spectroscopy has been widely used to explore chemical interactions at solid−liquid interfaces for biological, nonbiological, organic, or inorganic samples.[21] In the current study, this method was used as a nondestructive technique to investigate chemical bonds formed between the above-mentioned materials and ZnO NP or Zn^{2+}. This approach could provide information for cross-comparisons between binding of ZnO NPs and Zn^{2+} to Chelex-100 and Metsorb and to elucidate the underlying differences.

EXPERIMENTAL SECTION

2. MATERIAL AND METHODS

2.1. Chemicals. ZnO NPs were obtained from a commercial supplier (30 nm ZnO powder Nanosun without surfactant).[22] Point of zero charge for these NPs is approximately 6.5.[22] Chelex-100 and Metsorb were respectively purchased from Bio-Rad and Graver Technologies. Prior to each test, a fresh stock of ZnO NP dispersion was prepared by adding 200 mg of powder ZnO NPs to 1 L of Milli-Q water followed by sonicating for at least 15 min. Fresh stock of Zn^{2+} solutions was also prepared by dissolving Sigma-Aldrich reagent grade $Zn(NO_3)_2$ in Milli-Q water.

2.2. Sample Preparations. Triplicate samples for each experimental treatment toward ATR-FTIR spectrochemical analysis were prepared. For this, 0.5 g of pure Chelex-100 or Metsorb (binding materials) was exposed to 20.0 mL of 1000.0 μg/L of one of four different treatments; ZnO NPs, Zn^{2+}, acidified Zn^{2+} solution and nonacidified mixture of ZnO NPs and Zn^{2+} (500 μg/L each) in triplicates. These high concentrations were necessary to enable detection by ATR-FTIR spectroscopy so that a binding mechanism could be established. In total five classes were prepared for each of the binding materials and included (1) blank binding agent (i.e., Chelex-100 or Metsorb); (2) exposure to ZnO NP; (3) exposure to Zn^{2+}; (4) exposure to mixture of ZnO and Zn^{2+} (all pH ≈ 6.2); and, (5) exposure to acidified Zn^{2+} with pH ≈ 4.5 (Table 1). The experiment's pH was approximately 4.5 for the acidified solution (obtained by adding concentrated ultrapure nitric acid) and ≈6.2 for other tests (initial pH of the suspension/solution without further adjustment). The samples were shaken for 3 h on a rotary shaker at 150 rpm, centrifuged for 15 min at 3500 rpm and then supernatant was discarded. To wash the samples, 50 mL of Milli-Q water was added to each of the test tubes, shaken for 5 min and centrifuged as before. The washing stage was repeated three times to remove residuals of nonchemically retained ZnO NPs, which could interfere with the bound NPs on the binding materials.

Table 1. Chelex®-100 and Metsorb Treatments and Their Corresponding Spectral Class and Group Number

spectal class number	group name	Chelex-100 and metsorb treatments	pH
1	A	blank Chelex-100 and Metsorb	≈6.2
2	A	exposed to ZnO NP	≈6.2
3	B	exposed to Zn^{2+}	≈6.2
4	B	treated with mixture of ZnO and Zn^{2+}	≈6.2
5	A	exposed to acidified Zn^{2+}	≈4.5

Then the binding agents were dried under pressurized nitrogen gas pressure, 0.4 bar, and a small portion of each dry sample was put on an infrared (IR) Low-E reflective glass slide for ATR-FTIR spectroscopy analysis (Figure 1). The amount of the prepared samples was enough to completely cover the ATR-FTIR crystal and provide required thickness (>3 μm) to eliminate supporting substrate (i.e., the glass slide) interference with the sample spectra.

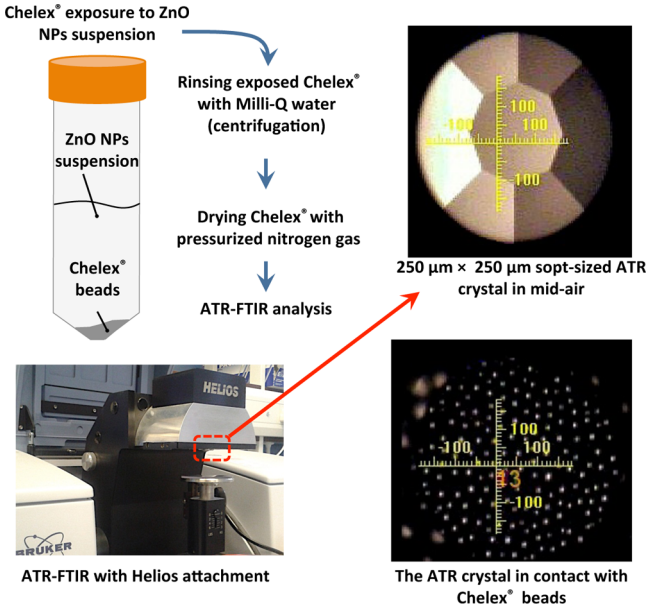

Figure 1. Schematic representation of the experimental procedure. Exposing Chelex-100 and Metsorb to ZnO NPs and Zn^{2+} suspensions and solution for spectral acquisition.

2.3. Spectra Acquisition and Data Processing. A Bruker Tensor 27 FTIR with Helios attachment containing diamond

dx.doi.org/10.1021/es4017552 | Environ. Sci. Technol. 2013, 47, 11115−11121

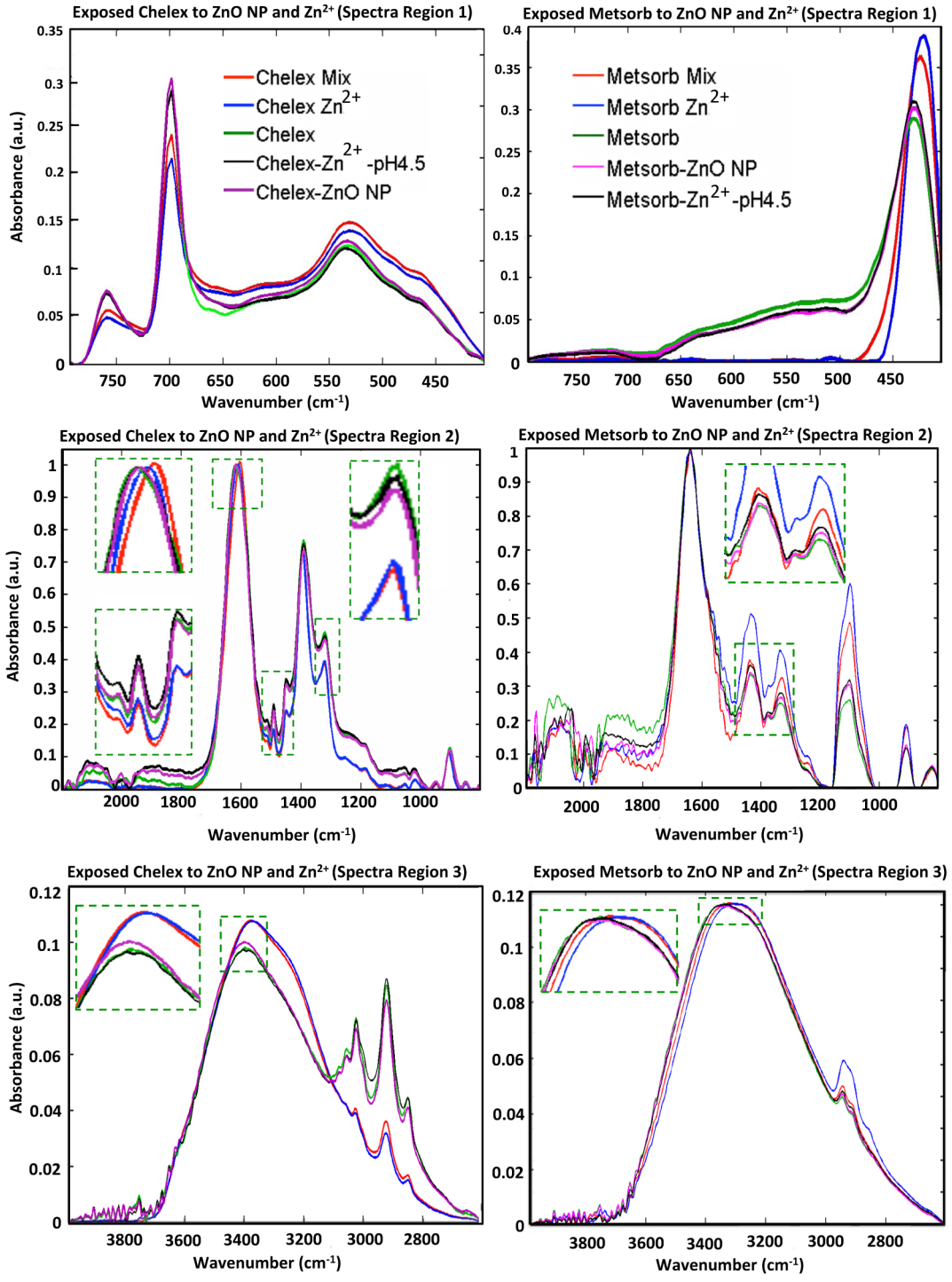

Figure 2. Comparison between derived infrared (IR) spectra for Chelex-100 and Metsorb exposed to ZnO NP and Zn^{2+}. The IR spectra (400−4000 cm^{-1}) is divided into three spectral regions: region 1 (400−800 cm^{-1}), region 2 (800−2200 cm^{-1}), and region 3 (2600−4000 cm^{-1}) for comparison purpose.

ATR Internal Reflection Element (IRE) was used for data acquisitions (Bruker Optics Ltd., Coventry, UK). Each experiment was conducted in triplicate and for each sample, 10 spectra were acquired at 4 cm^{-1} spectral resolution. Raw IR spectral data (400−4000 cm^{-1}) was cut to different spectral ranges: region one, 400−800 cm^{-1}; region two, 800−2200 cm^{-1}; and, region three, 2600−4000 cm^{-1}. Baseline correction (rubber band) and vector normalization was employed for all the regions.

Following processing, spectral data were then analyzed using principal component analysis (PCA) coupled with linear discriminating analysis (LDA), thus PCA-LDA. PCA is used to reduce the number of variables in spectral data (i.e., absorbance intensities at different wavenumbers) to only few factors (typically less than 10 factors) that can capture >95% variance of the data set. When the within-class variation is larger than that found between classes, LDA may be applied to the output from PCA.[25] This minimizes the within-class variation

and maximizes between-class variation allowing the identification of most important discriminating information and removing interference from the data. Thus, this approach allows for identification of class differences through the generation of scores and loadings plots. In the LDA scores plot, each spectrum becomes a point in LDA space and classes tend to form clusters where the closeness between points implies spectral similarities and distance signifies class dissimilarities. In addition, loadings plots can be used to identify chemical bonds distinguishing different treatment conditions.

3. RESULTS AND DISCUSSION

Different regions of IR spectra derived from Chelex-100 and Metsorb following their exposure to the different experimental conditions are shown in Figure 2.

As described (also in Table 1), there are five spectral classes. Based on the IR absorbance results of spectral peak intensities for Chelex-100 and Metsorb, they could be divided in two groups: A and B. Group A is the blank binding material, exposed to ZnO NPs and treated with Zn^{2+} (acidic pH) spectral classes 1, 2, and 5; and, group B includes the binding agent exposed to Zn^{2+} and a mixture of Zn^{2+} with ZnO NPs, spectral classes 3 and 4 (Table 1).

Before explaining the underlying phenomena that may have led to these differences, it is worth pointing out that even within each group, clear alterations are observed in different peak absorbance intensities or shifts in wavenumbers. Chelex-100 and Metsorb possess the ability to bind cations because of their surface functional groups.[3,23] Chelex-100 carboxyl and Metsorb surface titanium oxide/hydroxide hydroxyl group can bind available Zn^{2+} and ZnO NPs and irreversibly retain them.

Figure 3 is a schematic representation of potential chemical bonding that may occur between the binding agents and Zn^{2+} or ZnO NPs. As already stated, deprotonation of carboxyl groups in Chelex-100 occurs in pH ≈ 4.0 and point of zero charge for Metsorb is pH ≈ 6.0, hence, their overall surface charge in the pH ≈ 6.2 experiment is negative for Chelex-100 and neutral to slightly negative for Metsorb. When acidified at pH ≈ 4.5, Chelex-100 has a negative while Metsorb expresses a positive surface charge. At any given pH, protonated and deprotonated functional groups exist on the resin surface but their ratio is affected by the concentration of protons.[24]

Regardless of pH of the experiments, the primary binding behavior of Chelex-100 and Metsorb, when exposed to Zn^{2+} and ZnO NPs, can be predicted.

A carboxyl group following deprotonation could bind Zn^{2+} directly and two adjacent carboxyl groups are able to chemisorb Zn^{2+} cation while hydroxyl and carbonyl groups together could form a complex with Zn^{2+}. ZnO NP is a metal oxide with protonated and deprotonated surface hydroxyl groups (PZC ≈ 6.5). When exposed to a carboxyl group, a chemical bond could form between protonated ZnO NP surface hydroxyl groups and deprotonated carboxyl. Other bindings between structural Zn at the surface of ZnO NP and carboxyl carbonyl and hydroxyl groups are also possible.

Metsorb (titanium oxide) surface deprotonated hydroxyl groups form chemical bonds with Zn^{2+}. For ZnO NPs, Metsorb protonated and deprotonated surface hydroxyl groups could form hydrogen bonds with ZnO deprotonated and protonated surface hydroxyl groups. Two adjacent surface hydroxyl groups could also form hydrogen bonds between the two surfaces. Other possibilities include electrostatic attraction between

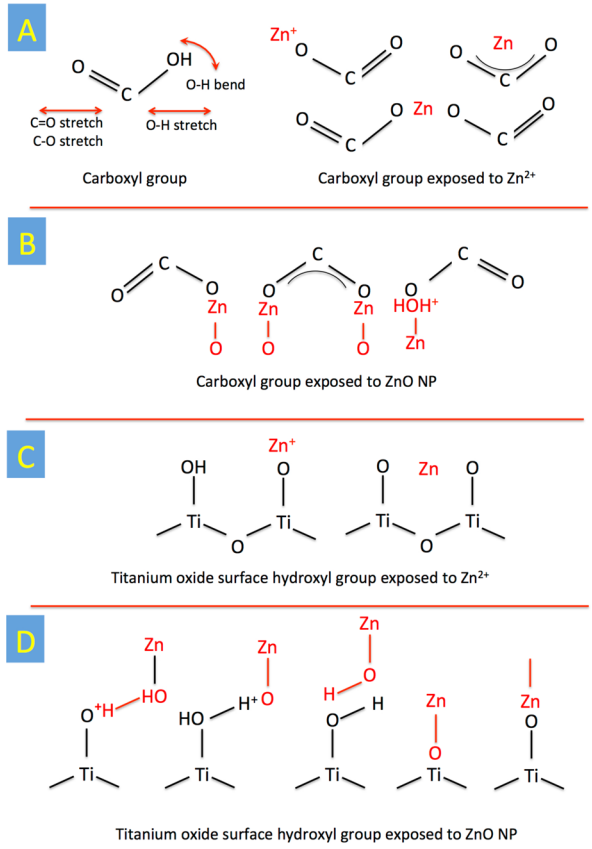

Figure 3. Schematic representation of some of major chemical bonds that could form between Chelex-100 carboxylgroup with Zn^{2+} (A) and ZnO NP (B) or Metsorb hydroxyl group with Zn^{2+} (C) and ZnO NP (D).

structural titanium of Metsorb and oxygen of ZnO NPs (from surface hydroxyl deprotonation or structural) or surface oxygen of titanium oxide (deprotonated hydroxyl group or structural) with structural Zn of ZnO NP. In spectra derived following ATR-FTIR spectroscopy, each of above-mentioned bond formation possibilities would reflect vibrational changes for chemicals involved in the reaction.[21,25] Figure 2 examines IR spectra of these chemicals in more detail.

In spectral region one (400−800 cm^{-1}), Chelex-100 treatments result in three major alterations at ≈530 cm^{-1}, ≈700 cm^{-1}, and ≈760 cm^{-1} with clear distinction (peak intensities and shift in wavenumbers) between the group A and B (Zn^{2+} and its mixture with ZnO NPs spectra). These peaks can be assigned to C−N−C, C−H, and N−H vibrations,[26] respectively. For Metsorb, shifts in peak wavenumbers are clearer. The skewed broad peak that is extended from ≈400 cm^{-1} and ≈700 cm^{-1} can be attributed to metal oxygen bond vibrations that are present in the titanium oxide in Metsorb.[27] In addition to differences in peak intensities, Metsorb exposed to Zn^{2+} or its mixture with ZnO NPs give rise to relatively sharper peaks compared to other Metsorb treatments, which may be as a result of hydrogen bond formation of hydroxyl groups.[26]

In spectral region two, Chelex-100 treatments give rise to alterations at ≈900 cm^{-1} (C−H out-of-plane bending), ≈1330 cm^{-1} (O−C stretching), ≈1400 cm^{-1} (C−O−H in plane bending), ≈1430 cm^{-1} (O═C−O stretching of carboxylate group), ≈1500 cm^{-1} (N−H bending), and ≈1620 cm^{-1} (C═O stretching).[26] As observed, groups one and two IR spectra show

dx.doi.org/10.1021/es4017552 | Environ. Sci. Technol. 2013, 47, 11115−11121

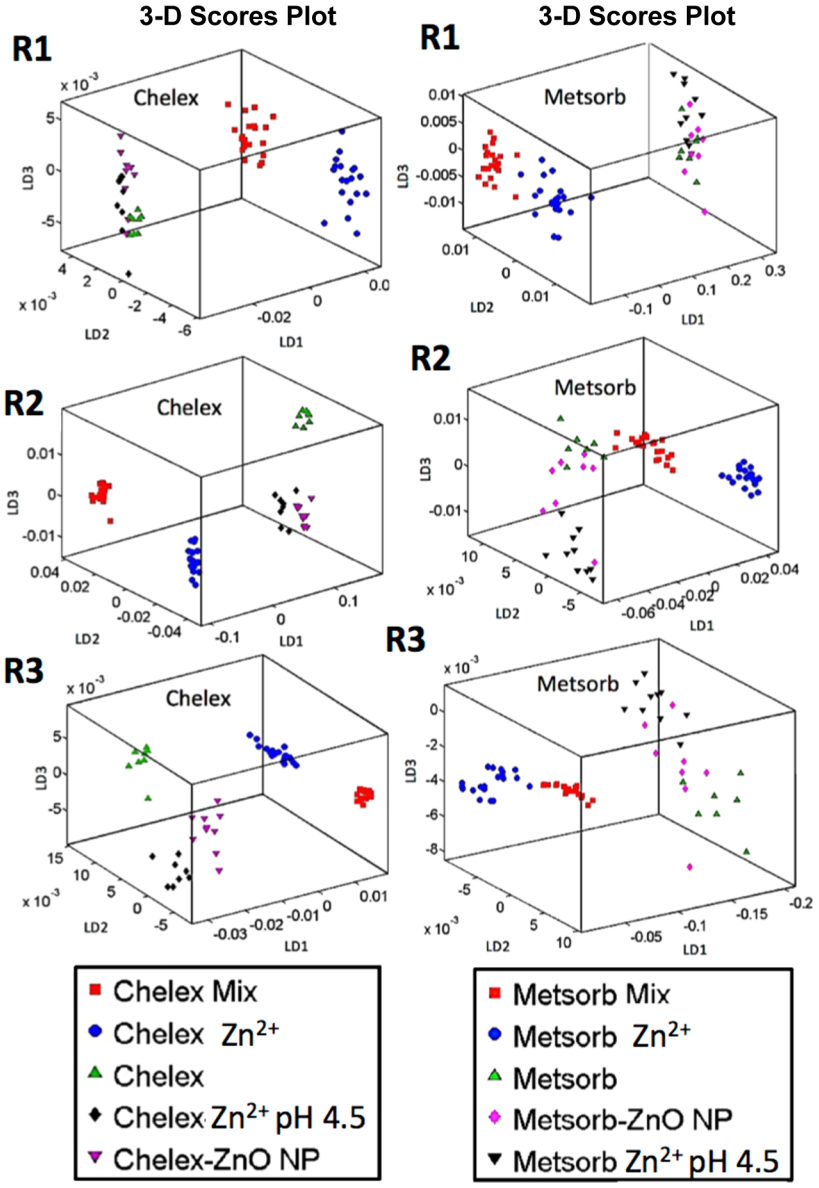

Figure 4. Three-dimensional scores plot visualization of principal component analysis and linear discriminant analysis (PCA-LDA) of Chelex-100 and Metsorb when exposed to ZnO NP and Zn^{2+}. R1 (400−800 cm^{-1}), R2 (800−2200 cm^{-1}), and R3 (2600−4000 cm^{-1}), respectively, represent three spectral regions of the spectra. Scales for *X*, *Y*, and *Z*-axis are arbitrary units.

different peak intensities for ≈1330 cm^{-1} and ≈1430 cm^{-1} and shifts in peak wavenumber ≈1620 cm^{-1}. These changes could reflect differences in strength of chemical bond formation between oxygen (from C−O, O═C−O, and C═O) and Zn^{2+} or structural Zn of ZnO NP or its surface hydroxyl groups. As already mentioned, Metsorb is not purely a titanium oxide compound and has some impurities including ethenal (C_2H_4O).[8] In region two, Metsorb spectra exhibits bands at ≈1100 cm^{-1}, ≈1350 cm^{-1} and ≈1440 cm^{-1} that could be assigned to C−OH stretch, C−OH, and O−H in-plane bend, respectively.[26] Comparing these peaks for the two groups of treatments indicate involvement of surface hydroxyl groups in bond formation with Zn^{2+} and/or ZnO NPs. The band at ≈1650 cm^{-1} is likely because of the bending mode of H−O−H. Absorbance of water or protonation of surface hydroxyl groups could both cause this vibrations.[28]

In region three, Chelex-100 spectra exhibit a broad O−H stretch peak that spans from ≈2800 cm^{-1} to ≈3600 cm^{-1}. Stretching vibrations of N−H at ≈3400 cm^{-1} may also contribute to this peak. Multiple bands at ≈2850 cm^{-1}, ≈2920 cm^{-1} and ≈3030 cm^{-1} are possibly a result of symmetric and asymmetric stretching of C−H and =C−H stretching.[21] In this region, Metsorb exhibits a broad peak at ≈3100−3600 cm^{-1} that is due to O−H stretching. This peak has a shoulder at ≈2950 cm^{-1} that is likely caused by Ti−OH bending.[27] Differences in electrostatic attractions between Zn^{2+} and structural Zn or oxygen of ZnO NP or its surface hydroxyl group with functional groups of these vibrational bands is likely the reason for changes in intensities and shifts in these wavenumbers.

A 3-D scores plot that shows PCA-LDA of absorbance spectra from Chelex-100 and Metsorb is presented in Figure 4. Details of this computational analysis approach are available in other publications.[29−32] As shown in this figure, two groups can also be distinguished following multivariate analysis, where in group one spectra, a segregation of the binding agent exposed

dx.doi.org/10.1021/es4017552 | *Environ. Sci. Technol.* 2013, 47, 11115−11121

to Zn^{2+} or a mixture of Zn^{2+} with ZnO NPs is observed, and in group two spectra, the blank binding material, treated with Zn^{2+} (acidic pH) and exposed to ZnO NPs created the second cluster; this separation is apparent in both Chelex-100 and Metsorb samples. Components of each of these groups have clear differences with each other. The 3-D scatter plot separates derived IR spectra based on their characteristic differences in their absorbance. Derived spectra for Chelex-100 and Metsorb exposed to Zn^{2+} and a mixture of ZnO NP with Zn^{2+} are statistically different at the 95% confidence level (Supporting Information (SI)). However, the differences are less marked then their difference from the spectra of blank binding material, treated with Zn^{2+} (acidic pH) and exposed to ZnO NPs. Especially for Chelex-100, each of the total five treatments are different in nature, while for Metsorb treatments of the blank material, low pH Zn^{2+} and ZnO NP have diffused borders (see SI).

The strength and number of chemical bonds formed between functional groups of Chelex-100 or Metsorb and Zn^{2+} compared to ZnO NP are different. For Zn^{2+} they are attracting an easily available cation with a similar size while for ZnO NPs they are interacting with structural Zn or its surface hydroxyl groups. Available electrons of deprotonated functional groups are responsible for retaining Zn^{2+} by the binding resins. A lower pH results in more positive surface charge (i.e., less available binding sites) as for the experiments performed at ≈4.5. As shown in Figure 4, this results in clearly different spectra for the same binding resin exposed to Zn^{2+} in pH ≈ 4.5 compared to pH ≈ 6.2, with the former compatible to exposure to ZnO NPs. The differences between the observed IR spectra for group A and B (exposure to ZnO NP and Zn^{2+} as shown in Figure 2) include both decreased absorbance intensities and shifts in the wavenumber of peaks. Such alterations are often associated with the formation of stronger chemical bonds where their bound species have more restricted movement.[26] Similar behavior is observed for the binding resins exposed to Zn^{2+} versus ZnO NP. The assigned band wavenumbers for Zn^{2+} are noticeably shifted and reduced, which indicates stronger chemical bonds.[21] For Chelex-100, bands with wavenumbers ≈530, ≈700, ≈760, ≈1330, ≈1620, ≈2850, ≈2920, ≈3030, and ≈3400 cm^{-1} all exhibit distinctive shifts to lower frequency when exposed Zn^{2+} (group B) samples. For Metsorb, a similar pattern is seen for ≈420, ≈1100, ≈1350, ≈1440, and ≈3300 cm^{-1}. This suggests that ZnO NPs are retained by Chelex-100 or Metsorb less strongly compared to Zn^{2+} because of fewer and weaker chemical bonds.

This study confirms chemical bond formation between ZnO NP as a model metal oxide NP and the two commonly used binding resins, Chelex-100 and Metsorb, in diffusive gradients in thin-film (DGT) . It provides further evidence that the DGT technique potentially could be modified to measure NPs in the environment. In particular, ATR-FTIR spectroscopy in combination with computational analysis/pattern recognition method (e.g., PCA-LDA) and the DGT technique could be used as a reliable approach to identify different types of chemicals retained by a binding material. This feature could be considered as indirect method to determine presence of chemicals of interest in the environment.

■ ASSOCIATED CONTENT

Supporting Information

Two-dimensional visualization of principal component analysis and linear discriminant analysis (PCA-LDA) of Chelex-100 and Metsorb when exposed to ZnO NP or Zn^{2+}. This material is available free of charge via the Internet at http://pubs.acs.org.

■ AUTHOR INFORMATION

Corresponding Authors

*(H.M.P.) Phone: +44 7930342062; e-mail: hamidpouran@yahoo.com.

*(H.Z.) Phone: +44 1524 593899; e-mail: h.zhang@lancaster.ac.uk.

Notes

The authors declare no competing financial interest.

■ ACKNOWLEDGMENTS

This work was funded by a Natural Environment Research Council Grant NE/H013709/1 (U.K.), part of Transatlantic Initiative for Nanotechnology and the Environment. We thank the reviewers for their helpful comments on the manuscript.

■ REFERENCES

(1) Zhang, H.; Davison, W.; Knight, B.; McGrath, S. In situ measurements of solution concentrations and fluxes of trace metals in soils using DGT. *Environ. Sci. Technol.* **1998**, *32* (5), 704−710.

(2) Zhang, H.; Davison, W. In situ speciation measurements. Using diffusive gradients in thin films (DGT) to determine inorganically and organically complexed metals. *Pure Appl. Chem.* **2001**, *73* (1), 9−15.

(3) Davison, W.; Zhang, H. Progress in understanding the use of diffusive gradients in thin films (DGT)—Back to basics. *Environ. Chem.* **2012**, *9* (1), 1−13.

(4) Zhang, H.; Davison, W. Diffusional characteristics of hydrogels used in DGT and DET techniques. *Anal. Chim. Acta* **1999**, *398* (2−3), 329−340.

(5) Huynh, T.; Zhang, H.; Noller, B. Evaluation and application of the diffusive gradients in thin films technique using a mixed-binding gel layer for measuring inorganic arsenic and metals in mining impacted water and soil. *Anal. Chem.* **2012**, *84* (22), 9988−9995.

(6) Hutchins, C. M.; Panther, J. G.; Teasdale, P. R.; Wang, F.; Stewart, R. R.; Bennett, W. W.; Zhao, H. Evaluation of a titanium dioxide-based DGT technique for measuring inorganic uranium species in fresh and marine waters. *Talanta* **2012**, *97*, 550−556.

(7) Van Der Veeken, P. L. R.; Pinheiro, J. P.; Van Leeuwen, H. P. Metal speciation by DGT/DET in colloidal complex systems. *Environ. Sci. Technol.* **2008**, *42* (23), 8835−8840.

(8) Bio-RAD Chelex 100 and Chelex 20 chelating ion exchange resin instruction manual, 2012. http://www.bio-rad.com/webmaster/pdfs/9184_Chelex.PDF.

(9) GraverTechnologiesMetsorb MSDS. http://gravertech.com/PDF/MetSorb/lit/metsorb-msds-hmrg.pdf (2012).

(10) Sugimoto, T.; Zhou, X. P. Synthesis of uniform anatase TiO2 nanoparticles by the gel-sol method—2. Adsorption of OH- ions to Ti(OH)(4) gel and TiO_2 particles. *J. Colloid Interface Sci.* **2002**, *252* (2), 347−353.

(11) Zhu, X. L.; Yuan, C. W.; Bao, Y. C.; Yang, J. H.; Wu, Y. Z. Photocatalytic degradation of pesticide pyridaben on TiO_2 particles. *J. Mol. Catal. A-Chem.* **2005**, *229* (1−2), 95−105.

(12) Panther, J. G.; Teasdale, P. R.; Bennett, W. W.; Welsh, D. T.; Zhao, H. J. Titanium dioxide-based DGT technique for in situ measurement of dissolved reactive phosphorus in fresh and marine waters. *Environ. Sci. Technol.* **2010**, *44* (24), 9419−9424.

(13) Bennett, W. W.; Teasdale, P. R.; Panther, J. G.; Welsh, D. T.; Jolley, D. F. New Diffusive Gradients in a Thin Film Technique for Measuring Inorganic Arsenic and Selenium(IV) Using a Titanium Dioxide Based Adsorbent. *Anal. Chem.* **2010**, *82* (17), 7401−7407.

(14) Turner, G. S. C.; Mills, G. A.; Teasdale, P. R.; Burnett, J. L.; Amos, S.; Fones, G. R. Evaluation of DGT techniques for measuring inorganic uranium species in natural waters: Interferences, deployment time and speciation. *Anal. Chim. Acta* **2012**, *739*, 37−46.

(15) Gottschalk, F.; Nowack, B. The release of engineered nanomaterials to the environment. *J Environ Monit.* **2011**, *13* (5), 1145−1155.
(16) Gottschalk, F.; Sonderer, T.; Scholz, R. W.; Nowack, B. Modeled environmental concentrations of engineered nanomaterials (TiO_2, ZnO, Ag, CNT, fullerenes) for different regions. *Environ. Sci. Technol.* **2009**, *43* (24), 9216−9222.
(17) Mu, H.; Chen, Y. Long-term effect of ZnO nanoparticles on waste activated sludge anaerobic digestion. *Water Res.* **2011**, *45* (17), 5612−5620.
(18) Reed, R. B.; Ladner, D. A.; Higgins, C. P.; Westerhoff, P.; Ranville, J. F. Solubility of nano-zinc oxide in environmentally and biologically important matrices. *Environ. Toxicol. Chem.* **2012**, *31* (1), 93−99.
(19) Lin, D. H.; Xing, B. S. Phytotoxicity of nanoparticles: Inhibition of seed germination and root growth. *Environ. Pollut.* **2007**, *150* (2), 243−250.
(20) Nel, A. E.; Madler, L.; Velegol, D.; Xia, T.; Hoek, E. M. V.; Somasundaran, P.; Klaessig, F.; Castranova, V.; Thompson, M. Understanding biophysicochemical interactions at the nano-bio interface. *Nat. Mater.* **2009**, *8* (7), 543−557.
(21) Ojeda, J. J.; Romero-Gonzales, M. E.; Pouran, H. M.; Banwart, S. A. In situ monitoring of the biofilm formation of *Pseudomonas putida* on hematite using flow-cell ATR-FTIR spectroscopy to investigate the formation of inner-sphere bonds between the bacteria and the mineral. *Mineral Mag.* **2008**, *72* (1), 101−106.
(22) Nanosun, M. *ZnO NP Product Application Sheet*; Micronisers, 2012.
(23) Panther, J. G.; Bennett, W. W.; Teasdale, P. R.; Welsh, D. T.; Zhao, H. J. DGT measurement of dissolved aluminum species in waters: Comparing Chelex-100 and titanium dioxide-based adsorbents. *Environ. Sci. Technol.* **2012**, *46* (4), 2267−2275.
(24) Stumm, W.; Morgan, J. J. *Aquatic Chemistry, Chemical Equilibria and Rates in Natural Waters*; 3rd ed.; Wiley-Interscience, 1996.
(25) Weisz, A. D.; Regazzoni, A. E.; Blesa, M. A. ATR-FTIR study of the stability trends of carboxylate complexes formed on the surface of titanium dioxide particles immersed in water. *Solid State Ionics* **2001**, *143* (1), 125−130.
(26) Stuart, B. *Infrared Spectroscopy Fundamentals And Applications*; Whiley, 2004.
(27) Gao, Y. F.; Masuda, Y.; Seo, W. S.; Ohta, H.; Koumoto, K. TiO_2 nanoparticles prepared using an aqueous peroxotitanate solutions. *Ceram. Int.* **2004**, *30* (7), 1365−1368.
(28) Kim, W. J.; Veriansyah, B.; Kim, J. D.; Oh, S. G. Formation of titanium hydroxide nanoparticles in supercritical carbon dioxide. *J. Ceram. Process Res.* **2008**, *9* (1), 88−92.
(29) Trevisan, J.; Angelov, P. P.; Carmichael, P. L.; Scott, A. D.; Martin, F. L. Extracting biological information with computational analysis of Fourier-transform infrared (FTIR) biospectroscopy datasets: Current practices to future perspectives. *Analyst* **2012**, *137* (14), 3202−3215.
(30) Llabjani, V.; Trevisan, J.; Jones, K. C.; Shore, R. F.; Martin, F. L. Binary mixture effects by PBDE congeners and PCB congeners in MCF-7 cells: biochemical alterations assessed by IR spectroscopy and multivariate analysis. *Environ. Sci. Technol.* **2010**, *44* (10), 3992−8.
(31) Martin, F. L.; Kelly, J. G.; Llabjani, V.; Martin-Hirsch, P. L.; Patel, I. I.; Trevisan, J.; Fullwood, N. J.; Walsh, M. J. Distinguishing cell types or populations based on the computational analysis of their infrared spectra. *Nat Prot.* **2010**, *5* (11), 1748−1760.
(32) Martin, F. L.; German, M. J.; Wit, E.; Fearn, T.; Ragavan, N.; Pollock, H. M. Identifying variables responsible for clustering in discriminant analysis of data from infrared microspectroscopy of a biological sample. *J. Comput. Biol.* **2007**, *14* (9), 1176−1184.